

Gamma-Ray Burst Afterglow emission with a decaying magnetic field

Elena Rossi & Martin J. Rees

Institute of Astronomy, University of Cambridge, Madingley Road, Cambridge CB3 0HA, England
e-mail:emr,mjr@ast.cam.ac.uk

2 December 2024

ABSTRACT

In models for gamma ray burst afterglows, it is normally assumed that the external shock strongly amplifies the magnetic field and that this field maintains a steady value throughout the shocked region. We discuss the effects of modifying this (probably simplistic) assumption. The observations are incompatible with a post-shock field that decays too rapidly. However if the field pervaded only a few percent of the total thickness of the shocked shell (and the electrons undergo only inverse Compton losses in the remainder) the models would be more compatible with the high external densities expected in star-forming regions. Afterglow observations in all wavebands, especially at radio wavelengths, could help to pin down the field structure.

Key words: Subject heading: Gamma-rays: burst — radiation mechanisms: nonthermal—magnetic field

1 INTRODUCTION

It is widely accepted that GRBs afterglow emission is due to nonthermal radiation mechanisms produced in relativistic shocks, as the ejected matter from a highly energetic explosion expands into the surrounding medium. With current facilities we can observe at photon energies up to 10 keV and the modeling of the observed lightcurves shows in general a predominance of synchrotron emission over inverse Compton scattering on the synchrotron photons. (Panaitescu & Kumar 2001 (hereafter PK01)). Only in one case, GRB000926, has a Compton component been inferred (Harrison et al 2001). This fact sets an upper limit on the density of the medium surrounding the explosion, whose properties can help us to unveil GRBs progenitors. In the standard framework the dynamics of the remnant expansion follows an adiabatic law. This behavior is expected when the electrons cannot cool on the expansion timescale or (even when they can) the bulk of the energy remains in relativistic protons and magnetic fields. The post shock magnetic field, necessary for the synchrotron emission, is mainly generated during the shock itself, because the shock compression of the pre-existing field alone would lead to a negligible magnetic energy per particle (e.g. Gruzinov 2001). The magnetic field is normally assumed to be uniform and its lengthscale to be of the order of the remnant scale. The electron energy distribution behind the expanding shock front is given by a power law, down to a minimum injection energy. Modeling eight afterglow lightcurves within this framework has resulted in a wide range of density from $\sim 10^{-3}$ to $\sim 27 \text{ cm}^{-3}$, strongly indicating a low density environment (PK01). This

is inconsistent with other independent observations placing GRBs birth in a star forming region: SN bumps in afterglow lightcurves (Bloom et al. 1999, Lazzati et al 2001), metal lines (Antonelli et al 2000, Piro et al 2000, Reeves et al 2002), afterglow localizations close to star forming regions (Bloom, Kulkarni, Djorgovski 2002, Jaunsen et al 2002) and estimations of high density environment from the temporal evolution of external column density (Lazzati & Perna 2002). Another remarkable inference from this model is that the fraction of internal energy given to electrons (ϵ_e) is always much higher than the fraction given to magnetic field (ϵ_b). This implies that the magnetic field is relatively weak and the Compton emission dominates the overall cooling of the electrons.

Recently many publications have investigated the somewhat poorly understood generation of magnetic field in strong relativistic collisionless shocks (e.g. Kazimura et al 1998, Gruzinov and Waxman 1998, Medvedev & Loeb 1999, Gruzinov 2001). Kazimura et al (1998) found generation of a small-scale quasi-static magnetic field; similar results were found by Gruzinov (2001) at small simulation times but his longer run shows that the field quickly decays by Landau damping; as a result synchrotron emission could be insignificant. Medvedev & Loeb (1999) found more reassuring results. Relativistic two-stream magnetic instability can, they claim, generate stable randomly oriented strong magnetic field in the plane of the collisionless shock front, so synchrotron emission is possible. These contradictory results show our ignorance of the possible acceleration process, and of how (or if) the magnetic fields are created there. These

uncertainties, coupled with the apparent problems with the standard model, motivate us to explore the consequences for afterglow emission of a different scenario, where the propagation of the magnetic field to large scale is disfavored.

In this paper we present this more general theory for the GRB afterglow emission (§2); our results (§3) suggest that even a small modification in the magnetic lengthscale could substantially raise the estimated external density, if data are modeled in this new framework. This would allow a consistent picture where a massive star is the progenitor of long GRBs, as well as having interesting implications for post-shock amplifications of magnetic fields.

2 SHORT MAGNETIC LENGTHSCALE THEORY

The assumption of a post shock magnetic field persisting during all the expansion time has three main consequences for the synchrotron (S) emission and spectrum. First the emitting region linear dimension is $R \simeq c \times t_{exp}$, where t_{exp} is the expansion time in the lab frame; this enters in the calculation of the observed peak flux F_p . Then the observed cooling frequency ν_c is computed using the Lorenz factor, γ_c , of the electrons that cool radiatively on a timescale equal to the remnant age. Finally the lengthscale for synchrotron self-absorption has to be compared with the dimension of the fireball in order to compute the observed absorption frequency ν_a . The only break frequency which is not affected by any assumption about the extension of the magnetic field, is the observed peak frequency ν_m , corresponding to the minimum random Lorentz factor γ_m : it depends crucially only on the fractions of internal energy given to electrons, ϵ_e , and given to the magnetic field ϵ_b . Throughout the entire emission volume electrons cool also via inverse Compton (IC) on the synchrotron photons (Self Synchrotron Compton: SSC). This cooling process dominates the electrons cooling if the Compton parameter $Y = L_{IC}/L_S$ (IC and S luminosity ratio) is greater than one. This happens if $\epsilon_b \ll \epsilon_e$ and current estimates find in most objects $\epsilon_b/\epsilon_e \sim 10^{-1} - 10^{-2}$, (Wijers & Galama 1999, Granot et al 1999, PK01).

If the magnetic field behind the shock persists for an average timescale of $t_b < t_{exp}$, its lengthscale is $\lambda \simeq c \times t_b < R$. In principle λ could depend on time, (for example, since at early times the shock is stronger, the processes that create the magnetic field could be more effective and delay the magnetic field decay. Therefore it could probably last longer than at later times). As already mentioned, we do not have any consolidated understanding of this process, so for simplicity we will assume throughout this paper that $\lambda/R = \delta$ is constant throughout the duration of the afterglow. At each time the emitting region is then divided in two zones (see Fig 1). The first zone (region A) is the layer with dimension λ just behind the shock front, where there are newly accelerated electrons and magnetic field: here electrons emit via S and SSC; the second zone (region B) of linear dimension $R - \lambda$, is filled by electrons that have just cooled by S and SSC emissions and that now Compton scatter the radiation coming from the first layer. We suppose that the newly accelerated electrons are advected with the flow; they produce synchrotron radiation only for a short time (with a cooling break therefore only at very high energies) in region A near

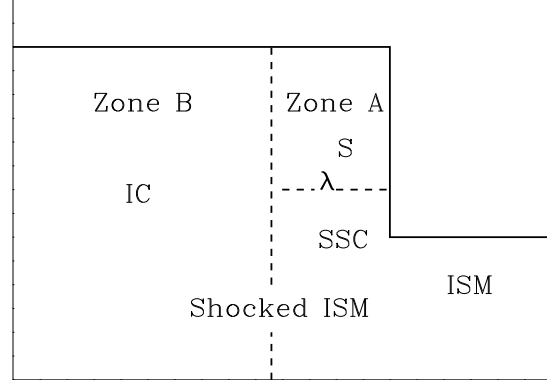


Figure 1. A schematic picture of the emitting region (shocked ISM). In region A, just behind the shock front, there are magnetic field and newly accelerated electrons that emit synchrotron and SSC for a time λ/c before downstreaming into the (unmagnetized) region B where they Compton scatter the S radiation coming from zone A.

the shock front and then they emit most of the IC radiation while downstreaming through region B. On the other hand if the electrons diffused freely, so that they could move back into the magnetized region after having lost most of their energy via IC, then the synchrotron spectrum would have a lower-energy break. This is probably less likely therefore we concentrate on the first case. The total observed spectrum then results from the sum of region A and region B spectra.

2.1 region A: S and SSC emission

The consequences of $\lambda < R$ on the S spectrum in region A can be derived easily from what we mentioned before. The observed peak frequency $\tilde{\nu}_m$ remains unchanged,

$$\tilde{\nu}_m = \nu_m, \quad (1)$$

and

$$\tilde{\gamma}_m \propto \tilde{\nu}_m^{1/2} = \gamma_m. \quad (2)$$

In our generalized model with $\delta < 1$ we denote quantities by the symbol ' \tilde{q} ', where ' q ' is defined for $\delta = 1$, (for the explicit definitions of quantities in the standard model we refer to Panaiteescu & Kumar 2000).

The comoving peak intensity is $I' \propto \tilde{n}' B' \lambda'$, where \tilde{n}' , B' and λ' are respectively the external density, the magnetic field and the emitting region linear dimension in the comoving frame; therefore the observed peak flux \tilde{F}_p is smaller than F_p by a factor δ :

$$\tilde{F}_p \simeq \Gamma^3 (\tilde{n}' B' \lambda') \frac{R^2}{\Gamma^2} = \delta \times F_p, \quad (3)$$

where Γ is the bulk Lorentz factor. Since the magnetic field persists for a shorter time, a smaller fraction of electrons cool significantly, before the magnetic field disappears in that region. The Lorentz factor of the electrons, whose cooling time is equal to the typical timescale of the system, $\tilde{\gamma}_c$ is therefore higher:

$$\tilde{\gamma}_c \propto \frac{1}{t_b' B'^2 (1 + \tilde{Y})} = \gamma_c \times \mathcal{Y} \delta^{-1}, \quad (4)$$

where $\mathcal{Y} = (1 + Y)/(1 + \tilde{Y})$. The observed cooling frequency $\tilde{\nu}_c \propto B' \tilde{\gamma}_c^2 \Gamma$ is then

$$\tilde{\nu}_c = \nu_c \times \mathcal{Y}^2 \delta^{-2}. \quad (5)$$

The synchrotron self-absorption optical thickness can be approximated as

$$\tilde{\tau}_a(\nu) \propto \left(\frac{\tilde{n} \lambda}{B' \tilde{\gamma}_p^5} \right) (\nu/\tilde{\nu}_p)^{-5/3} = \tilde{\tau}_p (\nu/\tilde{\nu}_p)^{-5/3}, \quad (6)$$

for $\nu < \tilde{\nu}_p$, where $p = c$ when the electrons are radiative ($\tilde{\gamma}_c < \tilde{\gamma}_m$) and $p = m$ when they are adiabatic ($\tilde{\gamma}_c > \tilde{\gamma}_m$). We will refer to the first case as fast-cooling regime and to the second case as slow-cooling regime. The absorption frequency corresponds to $\tilde{\tau}_a(\tilde{\nu}_a) = 1$ and in slow cooling regime is given by

$$\tilde{\nu}_a = \nu_a \times \delta^{3/5}, \quad (7)$$

where we use Eq. 1 and Eq. 6; in fast cooling regime Eqs 5, 6 and 18 ($\mathcal{Y} = 1$) give

$$\tilde{\nu}_a = \nu_a \times \delta^{8/5}. \quad (8)$$

Eqs 3, 7 and 8 are calculated in the case $\tilde{\nu}_a < \tilde{\nu}_p$ (see Granot & Sari 2001 for the different possible S spectra). Nevertheless $\tilde{\nu}_a \geq \tilde{\nu}_p$ for high densities

$$\tilde{n} \geq 7 \times 10^2 \delta^{-12/7} E_{53}^{-12/10} (1 + \tilde{Y})^{-3} \epsilon_{b,-2}^{-27/10} \quad (9)$$

in fast cooling and in slow cooling

$$\tilde{n} \geq 8.2 \times 10^5 \delta^{-1} E_{53}^{-1/2} \epsilon_{b,-2}^{1/2} \epsilon_{e,-2}^5 (1 + z) t_{day}^{5/2} \quad (10)$$

where E is the isotropic equivalent energy and t_{day} is the observed time in days. The inferred external density is reasonable for $\delta = 0.1$ ($\tilde{n} \geq 3.6 \times 10^4 \text{ cm}^{-3}$ and $\tilde{n} \geq 8.5 \times 10^6 t_{day}^{5/2} \text{ cm}^{-3}$ respectively) and for $\delta = 0.01$ ($\tilde{n} \geq 2 \times 10^6 \text{ cm}^{-3}$ and $\tilde{n} \geq 8.5 \times 10^7 t_{day}^{5/2} \text{ cm}^{-3}$) but for lower δ the density lower limits expressed in Eq 9 and Eq 10 are perhaps too high for the afterglow environment. For simplicity we focus thereafter on $\tilde{\nu}_a < \tilde{\nu}_c$ but the reader should keep in mind that these cases hold as long as Eq 9 and Eq 10 are not satisfied.

The magnetic energy $\frac{B'^2}{8\pi} \propto n\Gamma^2$ and the Compton parameter are higher at the beginning of the afterglow evolution and so the electrons are more likely then to be radiative. Since the minimum injected $\gamma_m \propto \Gamma$ decreases with time while γ_c increases as the efficiency of radiative loss decreases, the electrons undergo a transition to the adiabatic regime. The transition time between the fast cooling and the slow cooling regime is

$$\tilde{T}_{fs} = T_{fs} \times \delta^2; \quad (11)$$

for

$$\tilde{n} < 40 \delta^{-2} E_{53}^{-1} (Y_F + 1)^{-2} \epsilon_{B,-2}^{-2} \epsilon_{e,-1}^{-2} (1 + z)^{-1} t_{day}^{-1} \quad (12)$$

the slow-cooling regime dominates the fireball evolution during times when the afterglow is observed ($\gtrsim 1$ day).

The accelerated electrons that upscatter synchrotron photons give rise to a SSC component in the spectrum (for the SSC in the standard model see Sari & Asin 2000). During the afterglow phase the medium has a Thomson optical depth

$$\tilde{\tau} = \frac{1}{3} \tilde{n} \sigma_T R \delta \quad (13)$$

of the order of $\tilde{\tau} \simeq 10^{-5} \times \delta$ for $\tilde{n} = 10^2 \text{ cm}^{-3}$ (σ_T is the Thomson cross section), therefore only a minor fraction of the emission is upscattered, and the synchrotron flux is not significantly altered. Nevertheless if $\tilde{Y} \geq 1$ the electron cooling is Compton dominated and SSC upscatters low energy photons, that might be detected as a Compton component in x-ray and, in the future, in higher energy band spectra (Sari, Narayan & Piran 1996). The parameter \tilde{Y} can be defined as the mean number of scatterings times the average fractional energy change per scattering, gained by a photon traversing a finite medium (Rybicki & Lightman 1979). For a Thomson thin, relativistic medium \tilde{Y} is

$$\tilde{Y} \simeq \frac{4}{3} \tilde{\tau} \int \tilde{\gamma}^2 N(\tilde{\gamma}) d\tilde{\gamma} \quad (14)$$

where $N(\tilde{\gamma})$ is the normalized $\tilde{\gamma}$ distribution (see e.g. PK00 for explicit formulae for $\nu_a < \nu_p$). For $\tilde{Y} > 1$ one may need to consider more than one scattering per photon; however the energy of a photon in the rest frame of the second scattering electron is a factor γ^3 higher than the original energy, generally exceeding the Thompson regime limit (511 keV); the scattering cross section is then substantially reduced (Klein-Nishina (KN) regime) and further scatterings inhibited. As a consequence we will consider only single scattering of S photons. The KN effect limits also the electrons that mostly contribute to the SSC luminosity. They have a Lorentz factor

$$\tilde{\gamma} \leq \tilde{\gamma}_{KN} \simeq 511 \Gamma/h \tilde{\nu}_{Ep}, \quad (15)$$

where $\tilde{\nu}_{Ep}$ is the S energy peak frequency ($\tilde{\nu}_c$ in slow cooling and $\tilde{\nu}_m$ in fast cooling). In zone A the S spectrum can have a very high $\tilde{\nu}_c$ (see Eq 5); consequently in slow cooling $\tilde{\gamma}_c$ could be greater than $\tilde{\gamma}_{KN}$ and the Klein-Nishina effect substantially decreases \tilde{Y} (we will refer to this situation as “zone A in KN regime”). Moreover if $\tilde{Y} \simeq 1$ (which is the case in most simulations) we can omit the contribution from $\tilde{\gamma} > \tilde{\gamma}_{KN}$. Eq. 14 for $2 < p < 3$ gives then

$$\tilde{Y}_S (1 + \tilde{Y}_S)^{(3-p)} = Y_S (1 + Y_S)^{(3-p)} \times \delta^{(p-2)}, \quad (16)$$

for $\tilde{\gamma}_c \leq \tilde{\gamma}_{KN}$ and

$$\tilde{Y}_S (1 + \tilde{Y}_S)^{(2(p-3))} = Y_S (1 + Y_S)^{(2(p-3))} \times \delta^{(7-3p)}, \quad (17)$$

for $\tilde{\gamma}_c \leq \tilde{\gamma}_{KN}$. If the electrons are in the fast cooling regime it is very unlikely that $\tilde{\gamma}_m > \tilde{\gamma}_{KN}$ and Eq. 14 gives

$$\tilde{Y}_F = \frac{4}{3} \tilde{\tau} \tilde{\gamma}_m \tilde{\gamma}_c = Y_F; \quad (18)$$

note that \tilde{Y}_F does not depend on δ , because most of the electrons cool before the field disappears. Given a S seed spectrum $\tilde{F}_S(\nu_s)$, the resulting single scattering IC spectrum is (Rybicki & Lightman, 1979)

$$\tilde{F}_\nu^{IC} = A \int_0^1 \tilde{F}_S \left(\frac{\nu}{4\tilde{\gamma}^2 X} \right) f(X) dX \int_{\tilde{\gamma}_1}^{\tilde{\gamma}_2} N(\tilde{\gamma}) d\tilde{\gamma}, \quad (19)$$

where $A = 3\sigma_T R \delta$ (in this model), $X = \nu/4\tilde{\gamma}^2 \nu_s$ and $f(X) = 2X \ln X + X - 2X + 1$ includes the exact cross section angular dependence in the limit $\tilde{\gamma} \gg 1$ (Blumenthal and Gold, 1970). For the cases we are treating it is possible to use for the first integral the analytic expressions given by Sari & Asin (2000) in their Appendix A. The IC spectral peak flux and break frequencies for $\delta < 1$ are related to the IC spectrum for $\delta = 1$ in the following way

4 Rossi & Rees

$$\tilde{F}_p^{IC} \simeq \tilde{\tau} \tilde{F}_p = F_p^{IC} \times \delta^2 \quad (20)$$

using Eq 3 and Eq 6

$$\tilde{\nu}_m^{IC} \simeq 2\tilde{\gamma}_m^2 \tilde{\nu}_m = \nu_m^{IC}, \quad (21)$$

using Eq. 2, 1;

$$\tilde{\nu}_c^{IC} \simeq 2\tilde{\gamma}_c^2 \tilde{\nu}_c = \nu_c^{IC} \times (\mathcal{Y} \delta^{-1})^4, \quad (22)$$

using Eq. 4, 5;

$$\tilde{\nu}_a^{IC} \simeq 2\tilde{\gamma}_m^2 \tilde{\nu}_a = \nu_a^{IC} \times \delta^{3/5}, \quad (23)$$

in the slow cooling regime using Eq. 2, 7 and

$$\tilde{\nu}_a^{IC} \simeq 2\tilde{\gamma}_c^2 \tilde{\nu}_a = \nu_a^{IC} \times \delta^{-2/5} \quad (24)$$

in the fast cooling regime, using Eq. 4, 8.

2.2 Region B: IC emission

Zone B extends over a distance $(R - \lambda)$; since we are mainly interested in $\delta \leq 10^{-1}$, we approximate $(R - \lambda) \simeq R$ throughout this paper. This region is populated by electrons that have radiatively cooled via S and SSC for a time t_b . If they were originally injected at the front shock with a power-law energy distribution $N(\tilde{\gamma}) \propto \tilde{\gamma}^{-p}$ then the steady state distribution in region B depends on whether the electrons were adiabatic or radiative in region A. The $\tilde{\gamma}_{cB}$ for electrons that cool in a dynamical timescale t_{exp} is in fact

$$\tilde{\gamma}_{cB} = \frac{m_e c}{\frac{4}{3} \sigma_T \frac{U_{rad}}{2} t_{dyn}}, \quad (25)$$

where U_{rad} is the S radiation energy density and the factor 1/2 takes into account that only half of the S photons travel from region A towards region B in the electrons rest frame. The calculation of U_{rad} in the two different regimes leads to

$$\tilde{\gamma}_{cB} \propto \begin{cases} (n^2 e_b \Gamma \tilde{\gamma}^{p-1} \tilde{\gamma}_c^{3-p} R^2 \delta)^{-1} & \tilde{\gamma}_m < \tilde{\gamma}_c \\ (n^2 e_b \Gamma \tilde{\gamma}_m \tilde{\gamma}_c R^2 \delta)^{-1} & \tilde{\gamma}_m > \tilde{\gamma}_c \end{cases} \quad (26)$$

If electrons in region A are in the slow cooling regime, the new steady state configuration is

$$N(\tilde{\gamma}) \propto \begin{cases} \tilde{\gamma}^{-p} & \tilde{\gamma}_m < \tilde{\gamma} < \tilde{\gamma}_{cB} \\ \tilde{\gamma}^{-(p+1)} & \tilde{\gamma}_{cB} < \tilde{\gamma} < \tilde{\gamma}_c \\ \tilde{\gamma}^{-(p+2)} & \tilde{\gamma} > \tilde{\gamma}_c \end{cases} \quad (27)$$

for slow cooling ($\tilde{\gamma}_m < \tilde{\gamma}_{cB}$) or

$$N(\tilde{\gamma}) \propto \begin{cases} \tilde{\gamma}^{-2} & \tilde{\gamma}_{cB} < \tilde{\gamma} < \tilde{\gamma}_m \\ \tilde{\gamma}^{-(p+1)} & \tilde{\gamma}_m < \tilde{\gamma} < \tilde{\gamma}_c \\ \tilde{\gamma}^{-(p+2)} & \tilde{\gamma} > \tilde{\gamma}_c \end{cases} \quad (28)$$

for fast cooling ($\tilde{\gamma}_m > \tilde{\gamma}_{cB}$). $\tilde{\gamma}_{cB} > \tilde{\gamma}_c$ is very unlikely, even if the electrons in region A have two sources of energy loss (S and SSC), because $t_b < t_{exp}$ and SSC can be inhibited further for KN effect. If electrons in region A undergo fast cooling, the most common case is $\tilde{\gamma}_{cB} < \tilde{\gamma}_c$ and the new steady state configuration is

$$N(\tilde{\gamma}) \propto \begin{cases} \tilde{\gamma}^{-2} & \tilde{\gamma}_{cB} < \tilde{\gamma} < \tilde{\gamma}_c \\ \tilde{\gamma}^{-3} & \tilde{\gamma}_c < \tilde{\gamma} < \tilde{\gamma}_m \\ \tilde{\gamma}^{-(p+2)} & \tilde{\gamma} > \tilde{\gamma}_m \end{cases} \quad (29)$$

The “external Compton” spectrum in zone B is calculated by means of Eq 19 with $A = \frac{1}{2} \sigma_T R$ and the Compton parameter \tilde{Y}_B using Eq 14 and Eq 27- 29 with $\tilde{\tau}_B = \frac{\tau}{2}$.

Even if zone B has a higher number of IC emitting electrons, the Compton parameter can be lower than in region A: a higher fraction of the electrons in region B cool efficiently and they are in average less energetic than in region A, therefore increasing the density parameter \tilde{Y}_B decreases while \tilde{Y} increases because in zone A γ_c moves towards low values and the KN effect is less and less important (until the electrons become radiative and \tilde{Y}_F does not depend on density). In this situation the SSC radiation can actually account for most of the energy that goes into IC luminosity, (this is the case in Figs 2 and 3 right panels); anyway the SSC usually dominates the spectrum at high energy because it has a higher energy break. The peak flux is

$$\tilde{F}_p^{IC}(\nu) \simeq \tilde{\tau}_B \tilde{F}_p, \quad (30)$$

which is a factor $\delta^{-1}/2$ higher than \tilde{F}_p^{IC} in region A; while the spectral breaks are related to the S seed spectrum in slow cooling as follows

$$\tilde{\nu}_a^{IC} \simeq 2\tilde{\gamma}_m^2 \tilde{\nu}_a, \quad (31)$$

$$\tilde{\nu}_m^{IC} \simeq 2\tilde{\gamma}_m^2 \tilde{\nu}_m, \quad (32)$$

$$\tilde{\nu}_c^{IC} \simeq 2\tilde{\gamma}_{cB}^2 \tilde{\nu}_c, \quad (33)$$

if region B is in the slow cooling regime as well, and

$$\tilde{\nu}_a^{IC} \simeq 2\tilde{\gamma}_{cB}^2 \tilde{\nu}_a, \quad (34)$$

$$\tilde{\nu}_c^{IC} \simeq 2\tilde{\gamma}_m^2 \tilde{\nu}_c, \quad (35)$$

$$\tilde{\nu}_m^{IC} \simeq 2\tilde{\gamma}_{cB}^2 \tilde{\nu}_m, \quad (36)$$

if B is in the fast cooling regime. If S seed spectrum is in the fast cooling regime and $\tilde{\gamma}_{cB} < \tilde{\gamma}_c < \tilde{\gamma}_m$

$$\tilde{\nu}_a^{IC} \simeq 2\tilde{\gamma}_{cB}^2 \tilde{\nu}_a, \quad (37)$$

$$\tilde{\nu}_c^{IC} \simeq 2\tilde{\gamma}_{cB}^2 \tilde{\nu}_c, \quad (38)$$

$$\tilde{\nu}_m^{IC} \simeq 2\tilde{\gamma}_c^2 \tilde{\nu}_m. \quad (39)$$

3 DISCUSSION AND CONCLUSIONS

In Fig 2 and Fig. 3 left panels, we show as examples how the spectrum (respectively for fast and slow cooling) modifies if a short magnetic lengthscale is taken into account. Note that S and IC peak fluxes are lower (see also Eq. 3, Eq. 20, Eq. 30), a lower energy break corresponding to the absorption frequency is present (see Eqs. 7 and 8) and the cooling frequency is at higher energies (see Eq. 5). The SSC component in the slow cooling spectra of region A (Fig 2) is depleted because the KN effect is important. In the right panels we raise the density until $\tilde{F}_p \propto \tilde{n}^{1/2} \delta = F_p \propto n^{1/2}$, thus $\tilde{n} = \frac{n}{\delta^2}$. We obtain $\tilde{\nu}_c = \nu_c$ and the $\delta < 1$ spectrum fails to match the standard spectrum only at radio wavelengths. Such high densities, in fact, more than compensate the shorter magnetic lengthscale and $\tilde{\nu}_a$ becomes greater than ν_a . Another important feature is that the total (region A plus region B) \tilde{Y} parameter is never much higher than Y , even when Y corresponds to a density δ^2 lower; in fact when $\tilde{F}_p = F_p$, the main contribution to IC luminosity comes from region A and Eq 18 and Eq 16 hold: only \tilde{Y}_S depends on density and δ but the dependence are very weak ($\tilde{Y}_S (1 + \tilde{Y}_S)^{(3-p)} \propto \tilde{n}^{(p-2)/2} \times \delta^{(p-2)}$).

This “ δ model” and its consequences for the afterglow

emission apply to a uniform jet as well as to an inhomogeneous jet, where the energy per unit solid angle depends on the off-axis angle as $\epsilon \propto \theta^{-\alpha_\epsilon}$, with $\alpha_\epsilon \simeq 2$, (Rossi, Lazzati & Rees 2002). The results lead to very interesting conclusions. If the modeling succeeded in reproducing the data, a higher value for the external density ($\tilde{n} \geq 10^2$) would be derived, without an extreme IC component being observed. This could solve the discrepancy between the strong observational evidence that would place GRBs explosions in a star forming region and the low values for the environment densities, estimated by afterglow lightcurves modeling. However a *very* short scale magnetic field (say $\delta \lesssim 10^{-4}$) would be probably ruled out, since extremely high densities would be required in order to get fluxes in the observed ranges and the radio flux ($\nu < \tilde{\nu}_a$) would probably be too heavily absorbed: $\tilde{F}_\nu \propto \tilde{n}^{-1/2}$ (in adiabatic) and $\tilde{F}_\nu \propto \delta^{-1} \tilde{n}^{-5/3}$ (in radiative regime). On the other hand if this model failed in reproducing data, it could be either evidence in favor of an extremely stable field or the indication that some other modifications of the theory must be taken into account. If the former were true, it would strengthen the motivation to understand how relativistic shocks could amplify or generate a large scale and persistent magnetic field, a challenge that would reveal us more about relativistic shock physics. This work also highlights the importance of observing afterglows at all wavelengths, from radio to hard x-ray, and emphasizes that current estimations of the external density surrounding γ -ray bursts depend on uncertain details of shock physics.

ACKNOWLEDGMENTS

We thanks Davide Lazzati for the deep physical insight of his suggestions. ER thanks the Isaac Newton and PPARC for financial support.

REFERENCES

Antonelli, A., et al, 2000, ApJ, 545, L39
 Bloom J. S., Kulkarni S. R., Djorgovski S. G., et al., 1999, Nature, 401, 453.
 Bloom, J. S., Kulkarni, S. R., Djorgovski, S. G, 2002, AJ, 123, 1111
 Granot, J., Piran, T., & Sari, R., 1999, ApJ, 527, 236
 Gruzinov, A., 2001, ApJ, 563, L15
 Gruzinov, A., 2001, astroph/0111321
 Gruzinov, A., Waxman, E., 1999, ApJ, 511, 852
 Harrison, F. A., et al., 2001, ApJ, 559, 123
 Jaunsen, M. I., et al., 2002, astro-ph 0204278
 Lazzati, D. et al., 2001, A&A, 378, 996
 Lazzati, D., & Perna, R., 2002, MNRAS, 330, L383
 Medvedev, M., & Loeb, A., 1999, ApJ, 526, 697
 Panaiteescu A., Kumar P., 2000, ApJ, 543, 66
 Piro L., Garmire G., Garcia M., et al., 2000, Science, 290, 955.
 Panaiteescu A., Kumar P., 2001, ApJ, 560, L49 (PK01)
 Reeves, J.N. et al , 2002, Nature, 416, 512
 Reichart D. E., 1999, ApJ, 521, L111
 Rybicki, G. B., & Lightman, A. P., 1979, Radiative processes in astrophysics (New York: John Wiley & Sons)
 Rossi, E., Lazzati, D., & Rees, M. J., 2002, MNRAS in press, (astro-ph/0112083)
 Sari, R., & Esin, A.A., 2001, ApJ, 548, 787
 Sari, R., Narayan, R., & Piran, T., 1996, ApJ, 473, 204
 Wijers, R. A. M. J., & Galama, T. J., 1999, ApJ, 523, 177

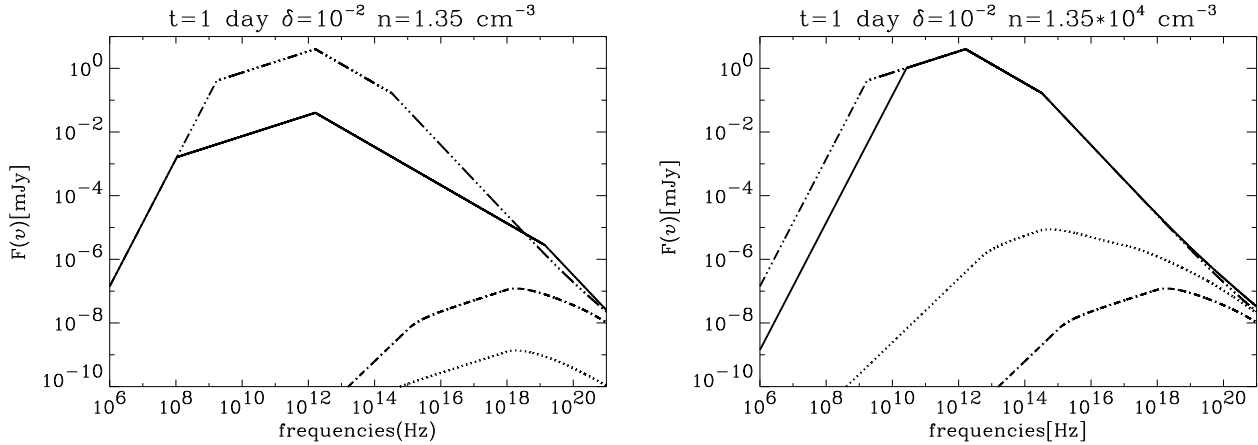


Figure 2. Total (solid line) and SSC+IC (dot line) spectra for $\delta = 0.01$ and total (3 dots-dash line) and SSC (dot-dash line) spectra for $\delta = 1$ at 1 day. In the left panel the two total spectra have all parameters, except for δ , the same: $n = 1.35 \text{ cm}^{-3}$, $E = 3 \times 10^{52} \text{ erg}$, $\epsilon_e = 6 \times 10^{-2}$, $\epsilon_B = 4 \times 10^{-3}$, $p = 2.2$ at a redshift $z = 1$. These parameters are typical of broadband afterglow lightcurves modeled in the standard framework (PK01). Both spectra are in the slow cooling regime (also zone B with $\gamma_{cB} < \gamma_c$). The SSC in zone A is highly inhibited by the KN effect; therefore most of the IC component is due to “external Compton” in zone B. The resulting Compton parameters are $\tilde{Y} = 0.40$ and $Y = 1.05$. In the right panel we raise the density in the $\delta = 0.01$ spectrum until $\tilde{F}_p = F_p$, $\tilde{n} = 1.35 \times 10^4 \text{ cm}^{-3}$. Zone B is now in the fast cooling regime therefore γ_{cB} moves towards low values but since in zone A the electrons are almost all in Thompson regime the total \tilde{Y} increases, $\tilde{Y} \simeq 1.10$: region A now dominates the IC emission. It is worth noticing that the two total spectra are distinguishable only in the radio waveband where the $\delta = 0.01$ flux is more absorbed.

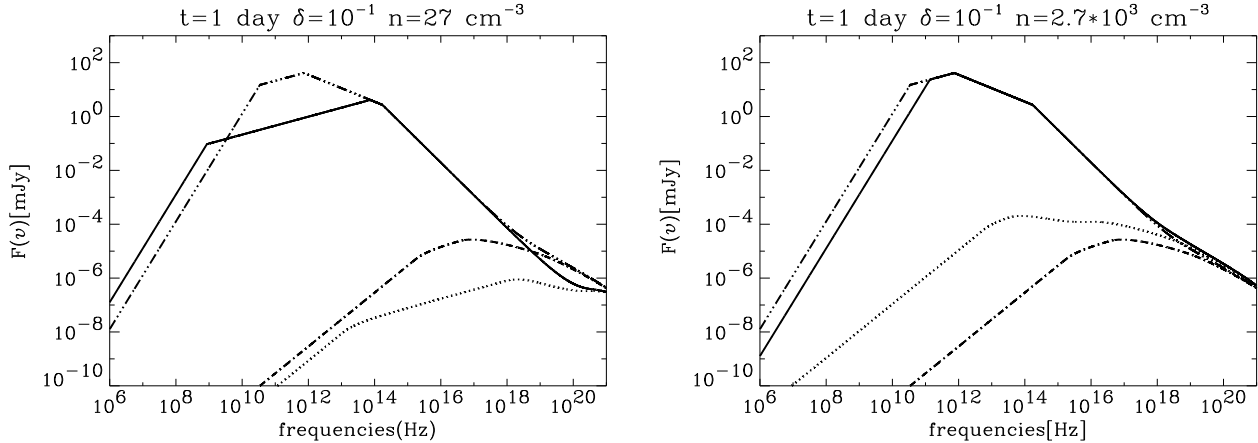


Figure 3. Same as Fig. 2 with parameters $n = 27 \text{ cm}^{-3}$, $E = 1.8 \times 10^{53} \text{ erg}$, $\epsilon_e = 0.3$ and $\epsilon_B = 8 \times 10^{-3}$ and $p = 2.43$ and $\delta = 0.1$. This set of parameters results from the best fit of 000926 (Harrison et al. 2001). The redshift of this burst is $z = 2.0639$. In the left panel both spectra are in fast cooling (also zone B with $\gamma_{cB} < \gamma_c$). The Compton parameters are $\tilde{Y} = 2.59$ and $Y_F = 2.34$. In the right panel we rise the value of density in the $\delta = 0.1$ spectrum until $\tilde{F}_p = F_p$, $\tilde{n} = 2.7 \times 10^3 \text{ cm}^{-3}$. The spectrum is obviously still in fast cooling with a lower γ_{cB} ; therefore the total \tilde{Y} is lower, $\tilde{Y} \simeq 2.37$ and the main contribution to the IC luminosity comes from region A. Again the two total spectra are distinguishable only in the radio waveband.